

# Field induced decrystallization of silicon: Evidence of a microwave non-thermal effect

Amin Nozariasbmarz,<sup>1,2,a)</sup> Kelvin Dsouza,<sup>1,a)</sup> and Daryoosh Vashaei<sup>1,2,b)</sup>

<sup>1</sup>Department of Electrical and Computer Engineering, North Carolina State University, Raleigh, North Carolina 27606, USA

<sup>2</sup>Department of Materials Science and Engineering, North Carolina State University, Raleigh, North Carolina 27606, USA

(Received 21 December 2017; accepted 9 February 2018; published online 26 February 2018)

It is rather strange and not fully understood that some materials decrystallize when exposed to microwave radiation, and it is still debatable if such a transformation is a thermal or non-thermal effect. We hereby report experimental evidences that weight the latter effect. First, a single crystal silicon wafer exposed to microwaves showed strong decrystallization at high temperature. Second, when some areas of the wafer were masked with metal coating, only the exposed areas underwent decrystallization. Transmission electron microscopy analysis, x-ray diffraction data, and thermal conductivity measurements all indicated strong decrystallization, which occurred in the bulk of the material and was not a surface effect. These observations favor the existence of a non-thermal microwave effect. *Published by AIP Publishing.* <https://doi.org/10.1063/1.5020192>

The interaction of microwave (MW) radiation with materials may be categorized into thermal and non-thermal effects.<sup>1</sup> The thermal effect contains different characteristics of dielectric heating. Compared to conventional heating, microwave heating is fast and uniformly heats up the dielectric material.<sup>1,2</sup> Microwave heating is a well-known process and is the operation principle of the existing kitchen and industrial microwave ovens. Overheating, hot spots, and selective heating are also considered as thermal effects.<sup>3</sup>

The non-thermal effect was perhaps first claimed by Gedye *et al.*<sup>4</sup> who reported different material responses due to microwave heating compared to conventional heating of similar thermal history<sup>5</sup> and was later associated with the inherent properties of the microwave radiation.<sup>6</sup> To date, the non-thermal effect is not yet quantifiable or verifiable.<sup>1</sup> The photons of the microwave radiation have energies in the range of  $10^{-5}$  to  $10^{-2}$  eV. This is only in the range of the quantum energy of dipole rotation and torsion. The energy of the chemical bonds is also much larger in the range of several eV's. Therefore, microwave radiation can only increase the temperature of a material by exciting the rotation and/or torsion of the dipoles. However, the thermodynamic of the process can be different from conventional heating.<sup>7-9</sup> For example, when the microwave radiation on a solid is terminated, the heating process instantly stops.<sup>10</sup> This process is known as field quenching, which results in the formation of metastable reaction products not accessible in conventional heating methods.<sup>1</sup>

The non-thermal effect has been mostly reported in organic chemistry,<sup>2,11-17</sup> while there are also some reports in solids.<sup>18-21</sup> For example, it has been shown that microwave heating can decrystallize oxides,<sup>19-22</sup> SiGe alloy,<sup>23</sup> and highly doped silicon,<sup>24</sup> which cannot be explained by equilibrium thermodynamic as heating normally causes grain growth and crystallization.

Several hypotheses have been made to explain the non-thermal effects such as inhomogeneous heating between grain boundaries and the bulk<sup>25</sup> and a non-thermal phonon distribution excited by microwave radiation.<sup>1,26</sup> However, the most persuading hypothesis is based on ponderomotive forces where the solid state ionic diffusion, particularly the mobility of the charged particles near the grain boundaries, increases due to the gradient of the high frequency electric field.<sup>5,27,28</sup>

The interaction of microwaves with valence electrons results in different trends of energy relaxation.<sup>29</sup> In comparison to conventional heating, the excited state of the valence electrons is dissimilar due to the monochromatic and single-phase nature of the microwave E- and H-fields. Hence, in addition to temperature, electronic charge and spin can also affect the degree of freedom for the internal energy. For instance, the reduction activation energy of oxides can be lowered by microwave radiation due to the increase in the internal energy.<sup>30</sup> Besides, the electromagnetic field can be efficiently converted into chemical energy without heat dissipation.<sup>31</sup> Therefore, in addition to conventional heating, microwave radiation can add some non-thermal energy to the electrons catalyzing certain chemical reactions. Furthermore, compared to the isotropic heating in conventional furnaces, the microwave energy in a single-mode cavity is anisotropic, which becomes isotropic after conversion into heat. Therefore, prior to energy relaxation, the anisotropic microwave energy can induce non-thermal effects such as the ones observed in the reduction of oxide materials.<sup>30</sup>

Despite the numerous experiments that indicate the existence of the microwave non-thermal effect, there are still counter arguments that completely reject the existence of the non-thermal effects and relate them to inaccurate temperature reading, thermal run-away, non-uniform heating of the material, or some experimental errors.<sup>2,3,32,33</sup>

This investigation presents evidences for the non-thermal effects. To reduce material related complexities, the experiments were performed on single crystal high purity

<sup>a)</sup>A. Nozariasbmarz and K. Dsouza contributed equally to this work.

<sup>b)</sup>Author to whom correspondence should be addressed: dvashae@ncsu.edu. Tel.: (919) 515-9599.

silicon wafers. The wafer rapidly decrystallized when exposed to a standing microwave radiation in a single mode cavity. Different characterization techniques including X-ray diffraction (XRD), transmission electron microscopy (TEM), and thermal conductivity analysis all indicated the decrystallization of the material. Furthermore, to eliminate the experimental ambiguities, as a control method, some part of the wafer was intentionally masked with a thick metal coating so that the electric field would not penetrate into the bulk of the sample in those regions. A pulsed microwave form was also used so that the temperature is distributed uniformly during the off times. It was found that after microwave radiation, the regions which were masked by metal were not decrystallized; however, the rest of the wafer was strongly decrystallized. These observations, which cannot be explained by equilibrium thermodynamics, support the existence of a non-thermal effect, the one still not fully understood.

All the experiments were done using a custom rectangular single-mode TE<sub>103</sub> microwave cavity with the maximum power of 1.2 kW at a frequency of 2.45 GHz. The samples were processed in a mixed electric field (E) and magnetic field (H). The radio frequency (RF) power was pulsed with a duty cycle of 90% to allow time for thermal equilibrium starting with a power of 60%, which increased gradually to 80%. The basic components of the system are a microwave source (magnetron), an isolator, tuners, a WR340 waveguide, an applicator, a sliding short, and a temperature monitoring system (pyrometer). The tuners and the sliding short were used for cavity adjustment and load matching. The temperature was monitored through a window next to the sample. The sample was placed in a magnesium oxide crucible and sealed inside a quartz tube under an argon atmosphere at approximately 700 Torr. Two groups of samples were radiated by microwaves. Group 1 was a pure single crystal silicon wafer with (400) surface orientation cut into rectangular bars of 10 mm × 5.8 mm × 1 mm. Group 2 was a pure single crystal silicon wafer with (400) surface orientation cut into rectangular bar of 12 mm × 6 mm × 0.7 mm. Half of the sample on both sides was coated with ~10 μm thick nickel using electron beam physical vapor deposition. This sample was used for selected area decrystallization studies.

The samples were exposed to pulsed microwave radiation with a period of 5 s and a duty cycle of 90% to allow for uniform volumetric heating. The sample was soaked at the maximum temperature of 850–1000 °C for approximately 5 min, and then, the microwave was turned off.

The processed samples were characterized by X-ray diffraction (XRD) using a Rigaku MiniFlex 600 with Cu-K<sub>α</sub> radiation apparatus at 2θ angles of 10°–80°. Transmission electron microscopy (TEM) and selected-area diffraction (SAD) analysis were performed using a JEOL 2010F operated at 200 kV with a current density of 20 pA/cm<sup>2</sup>. The thermal diffusivities (α) of the samples were measured using Linseis LFA 1000 Laser Flash, in the range of room temperature to 400 °C. The thermal conductivity (κ) was subsequently calculated according to  $\kappa = \alpha d C_p$ , where d is the mass density and C<sub>p</sub> is the specific heat.

The results are divided into two parts: (1) field-induced decrystallization of a single crystal silicon wafer and (2)

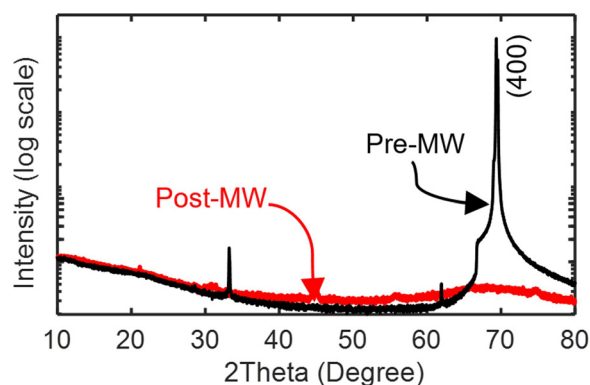


FIG. 1. XRD patterns of the silicon wafer before (pre-MW) and after (post-MW) microwave radiation.

selected-area decrystallization of the SC silicon wafer, which are explained below.

The XRD patterns of the pre- and post-microwave (MW) processed specimens are shown in Fig. 1. The pattern for the pre-MW sample shows a single high intensity diffraction peak of the (400) plane at  $2\theta = 69.3^\circ$ . The post-MW sample showed a significant reduction in the intensity of the same peak. Such a reduction in the peak intensity can be associated with the field induced randomness in the lattice arrangement after microwave radiation. It is speculated that the high temperature and high electric field of the microwave energy can provide adequate energy to dislodge the atoms from their lattice sites and diminish the long-range order of the crystals.

Figure 2(a) shows the high resolution TEM (HR-TEM) image and the corresponding SAD pattern of the pre-MW single crystal silicon. The SAD pattern confirms a single crystal structure in the  $[1\bar{1}2]$  zone axis. The corresponding TEM image displays uniform lattice fringes also indicating a single crystal structure.

Figure 2(b) shows the HR-TEM image and the SAD pattern of the post-MW single crystal silicon. The first, second, and third rings in the SAD pattern correspond to the diffraction of  $\{111\}$ ,  $\{220\}$ , and  $\{311\}$  planes, respectively. The image confirms the transformation of the single crystal silicon to a lattice disordered silicon, which consists of nanocrystals in the range of approximately 5 nm or less surrounded with amorphous regions.

To further confirm the field induced decrystallization and its effect on material properties, the thermal conductivity of the microwave processed samples was measured versus

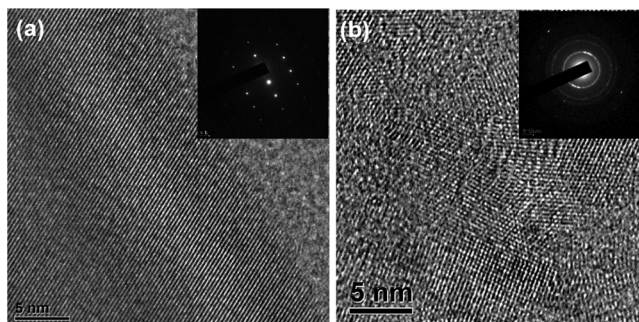


FIG. 2. High resolution TEM image and corresponding SAD pattern of the single crystal silicon wafer (a) before and (b) after microwave radiation.

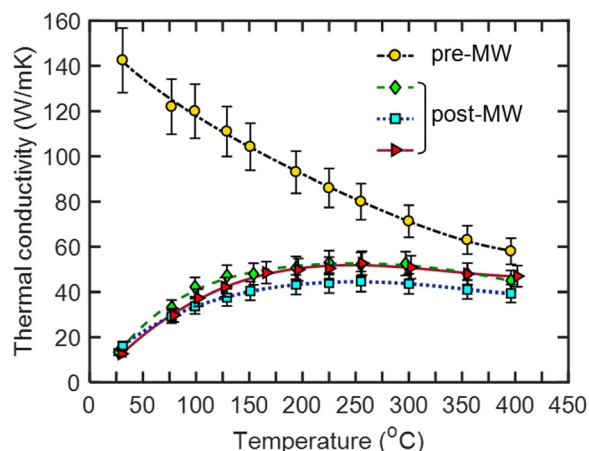


FIG. 3. Comparison of the thermal conductivity versus temperature of single crystal silicon wafers before (pre-MW) and after (post-MW) microwave radiation.

temperature. The result is shown in Fig. 3. The thermal conductivity of pre-MW follows the typical trend versus temperature for a single crystal silicon with a peak value of  $\sim 145$  W/mK at room temperature, which reduces with temperature due to 3-phonon scattering. However, all the microwave radiated samples (post-MW) show a significant reduction in the thermal conductivity near room temperature, which is due to the lattice defects such as nano-grains and amorphous domains that scatter the phonons.<sup>34</sup> The positive slope of the thermal conductivity versus temperature below  $\sim 300^\circ\text{C}$  in these samples is due to the phonon-grain boundary scattering which becomes less significant compared to 3-phonon scattering at higher temperature. As the temperature increases beyond  $300^\circ\text{C}$ , the 3-phonon scattering dominates, and the thermal conductivity follows the same trend as the pre-MW sample. The thermal conductivity of post-MW is higher than the predicted thermal conductivity of the amorphous silicon<sup>35</sup> and one eleventh of that of the single crystal silicon (pre-MW). It should be noted that at high temperature, the nano-scale features such as the small grains and amorphous regions diminish due to re-crystallization and the thermal conductivity converges to that of the pre-MW sample.

The possibility of selected-area decrystallization of a material, here Si wafer, was studied based on this concept. For this purpose, half of a Si wafer was coated with nickel and half was exposed as shown in Fig. 4. Then, the wafer was radiated with microwave under similar conditions as explained earlier. After the microwave radiation, the metal coating was etched, and the sample was cut into two separate pieces. The comparison of the XRD of the two pieces as shown in Fig. 4 indicates that the part covered with metal was not decrystallized. In contrast, the XRD of the microwave exposed part shows an amorphous hump in addition to the main diffraction peak, which is a character of a mixed amorphous crystalline phase.

In contrast to insulating dielectric materials, like ceramics, where the microwave field penetrates into the bulk of the material and heats it up through dielectric absorption, highly electrically conductive materials, like metals, are not internally affected by the microwave field. Instead, an induced alternating

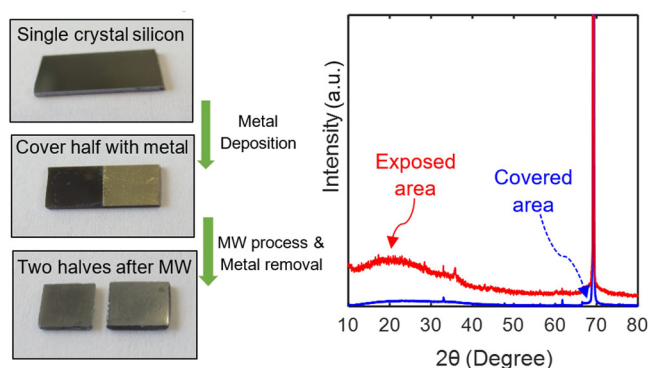


FIG. 4. Sample preparation and comparison of the XRD of the exposed and metal covered areas after microwave radiation.

electrical current is formed near the surface, which attenuates the penetrating field but enhances the reflected wave. The microwave penetration depth, also known as the skin depth ( $\delta$ ), can be estimated by  $\delta = \sqrt{\rho/\pi f \mu}$ , where  $f$ ,  $\mu$ , and  $\rho$  are the microwave frequency, magnetic permeability, and electrical resistivity of the metal, respectively.<sup>36,37</sup> Therefore, metals with very small electrical resistivity have a small microwave skin depth, and this amount increases with temperature (as  $\rho$  increases with temperature). The skin depth of nickel at 2.45 GHz is estimated to be  $\sim 2.7 \mu\text{m}$  at room temperature and  $\sim 7 \mu\text{m}$  at  $1000^\circ\text{C}$ , which is less than the thickness of the nickel film. Therefore, the microwave radiation did not directly interact with or heat the area under the metal. However, due to the joule heating in the skin layer, the surface of the metal heated up, and through conduction, the temperature of the Si layer increased underneath. The accurate temperature monitoring of the area under the nickel coating was not possible, but it is expected that the temperature of this part of the wafer also increases. As mentioned, the microwave radiation was periodically turned on and off so that the heat conduction during the off times should prevent hot spot formation and enhance the temperature uniformity across the sample.

Amorphization is thermodynamically an unfavorable process at equilibrium, and heating normally crystallizes the amorphous domains. The fact that the exposed area, which was heated directly by microwaves, is decrystallized while the metal covered area, which was shielded from radiation but heated indirectly, is not decrystallized evidences the existence of a non-thermal microwave effect. The decrystallization depth and strength are functions of process temperature and radiation time. These results indicate that it is possible to shield some areas of a sample with metal coating and prevent their decrystallization while the exposed regions are decrystallized by microwaves.

Although microwave radiation has been used extensively in materials processing, the existence of non-thermal microwave effects is still under debate. We hereby presented some experimental evidences that weight the existence of non-thermal microwave effects. It was shown that microwave energy can decrystallize single crystal silicon wafers. TEM images with selected-area diffraction patterns, macroscopic XRD analysis, and thermal conductivity measurements all indicated strong decrystallization of the wafer upon microwave radiation. In addition, by covering half of the wafer with a metal coating prior to microwave radiation,



it was shown that the coated area remained single crystal while the exposed area was decrystallized. Since both halves simultaneously experienced similar process conditions, the decrystallization indicates the existence of the non-thermal microwave effect.

This study is partially based upon the work supported by the Air Force Office of Scientific Research (AFOSR) under Contract No. FA9550-12-1-0225 and the National Science Foundation (NSF) under Grant Nos. EEC-1160483, ECCS-1351533, and CMMI-1363485. This work was performed in part at the Analytical Instrumentation Facility (AIF) at North Carolina State University, which is supported by the State of North Carolina and the National Science Foundation (award number ECCS-1542015). The AIF is a member of the North Carolina Research Triangle Nanotechnology Network (RTNN), a site in the National Nanotechnology Coordinated Infrastructure (NNCI).

- <sup>1</sup>H. J. Kitchen, S. R. Vallance, J. L. Kennedy, N. Tapia-Ruiz, L. Carassiti, A. Harrison, A. G. Whittaker, T. D. Drysdale, S. W. Kingman, and D. H. Gregory, *Chem. Rev.* **114**, 1170 (2014).
- <sup>2</sup>A. de la Hoz, Á. Díaz-Ortiz, and A. Moreno, *Chem. Soc. Rev.* **34**(2), 164 (2005).
- <sup>3</sup>J. Ma, *J. Phys. Chem. A* **120**, 7989 (2016).
- <sup>4</sup>R. Gedy, F. Smith, K. Westaway, H. Ali, L. Baldisera, L. Laberge, and J. Rousell, *Tetrahedron Lett.* **27**(3), 279 (1986).
- <sup>5</sup>Y. V. Bykov, K. I. Rybakov, and V. E. Semenov, *J. Phys. D: Appl. Phys.* **34**, R55 (2001).
- <sup>6</sup>S. A. Galema, *Chem. Soc. Rev.* **26**, 233 (1997).
- <sup>7</sup>J. W. Cable, *Introduction and Dielectric Heating* (Reinhold Publishing Corporation, New York, USA, 1954).
- <sup>8</sup>A. Nozariasbmarz, "In-situ sintering decrystallization of thermoelectric materials using microwave radiation," Ph.D. thesis (North Carolina State University, Raleigh, North Carolina, USA, 2017).
- <sup>9</sup>M. Willert-Porada, *Advances in Microwave and Radio Frequency Processing* (Springer-Verlag, Berlin, Heidelberg, 2006).
- <sup>10</sup>D. E. Clark and W. H. Sutton, *Annu. Rev. Mater. Sci.* **26**, 299 (1996).
- <sup>11</sup>C. Shibata, T. Kashim, and K. Ohuchi, *Jpn. J. Appl. Phys., Part 1* **35**, 316 (1996).
- <sup>12</sup>N. Kuhnert, *Angew. Chem., Int. Ed.* **41**, 1863 (2002).
- <sup>13</sup>A. Miklavc, *Chemphyschem* **2**, 552 (2001).
- <sup>14</sup>M. Porcelli, G. Cacciapuoti, S. Fusco, R. Massa, G. d'Ambrosio, C. Bertoldo, M. De Rosa, and V. Zappia, *FEBS Lett.* **402**, 102 (1997).
- <sup>15</sup>G. B. Dudley, R. Richert, and A. E. Stiegman, *Chem. Sci.* **6**, 2144 (2015).
- <sup>16</sup>M. Nuchter, B. Ondruschka, W. Bonrath, and A. Gum, *Green Chem.* **6**(3), 128–141 (2004).
- <sup>17</sup>M. Kanno, K. Nakamura, E. Kanai, K. Hoki, H. Kono, and M. Tanaka, *J. Phys. Chem. A* **116**(9), 2177 (2012).
- <sup>18</sup>R. Roy, D. Agrawal, J. Cheng, and S. Gedevarishvili, *Nature* **399**, 668 (1999).
- <sup>19</sup>R. Roy, R. Peelamedu, L. Hurtt, and J. Cheng, *Mater. Res. Innovations* **6**, 128 (2002).
- <sup>20</sup>R. Roy, Y. Feng, J. Cheng, and D. K. Agarwal, *J. Am. Ceram. Soc.* **88**, 1640 (2005).
- <sup>21</sup>R. Wroe and A. T. Rowley, *J. Mater. Sci.* **31**, 2019 (1996).
- <sup>22</sup>R. Peelamedu, R. Roy, L. Hurtt, D. Agrawal, A. W. Fliflet, D. Lewis III, and R. W. Bruce, *Mater. Chem. Phys.* **88**, 119 (2004).
- <sup>23</sup>J. Cheng, D. Agrawal, Y. Zhang, R. Roy, and A. K. Santra, *J. Alloys Compd.* **491**, 517 (2010).
- <sup>24</sup>R. Peelamedu, R. Roy, D. Agrawal, and W. Drawl, *J. Mater. Res.* **19**(6), 1599 (2004).
- <sup>25</sup>D. L. Johnson, *J. Am. Ceram. Soc.* **74**(4), 849 (1991).
- <sup>26</sup>J. H. Booske, R. F. Cooper, and I. Dobson, *J. Mater. Res.* **7**(2), 495 (1992).
- <sup>27</sup>K. I. Rybakov, E. A. Olevskaya, and V. E. Semenov, *Scr. Mater.* **66**, 1049 (2012).
- <sup>28</sup>J. H. Booske, R. F. Cooper, S. A. Freeman, K. I. Rybakov, and V. E. Semenov, *Phys. Plasmas* **5**(5), 1664 (1998).
- <sup>29</sup>J. Fukushima, K. Kashimura, and M. Sato, "Chemical bond cleavage induced by electron heating -Gas emission behavior of titanium-metalloid compounds (titanium nitride and oxide) in a microwave field," *Mater. Chem. Phys.* **131**, 178 (2011).
- <sup>30</sup>J. Fukushima, K. Kashimura, S. Takayama, M. Sato, S. Sano, Y. Hayash, and H. Takizawa, "In-situ kinetic study on non-thermal reduction reaction of CuO during microwave heating," *Mater. Lett.* **91**, 252 (2013).
- <sup>31</sup>T. Ohta, *Energy Technology: Systems and Frontier Conversion* (Elsevier Science, New York, 1994).
- <sup>32</sup>C. O. Kappe, B. Pieber, and D. Dallinger, *Angew. Chem., Int. Ed.* **52**, 1088 (2013).
- <sup>33</sup>E. T. Thostenson and T.-W. Chou, *Composites, Part A* **30**, 1055 (1999).
- <sup>34</sup>T. Maruyama and M. Harayama, *J. Nucl. Mater.* **195**, 44 (1992).
- <sup>35</sup>P. Norouzzadeh, A. Nozariasbmarz, J. S. Krasinski, and D. Vashae, *J. Appl. Phys.* **117**, 214303 (2015).
- <sup>36</sup>M. Gupta, E. Wong, and W. Leong, *Microwaves and Metals* (John Wiley & Sons, Hoboken, NJ, USA, 2007).
- <sup>37</sup>P. Mishra, A. Upadhyaya, and G. Sethi, "Modeling of microwave heating of particulate metals," *Metall. Mater. Trans. B* **37**, 839–845 (2006).